Proceedings 10th NUMGE 2023
10th European Conference on Numerical Methods in Geotechnical Engineering
Zdravkovic L, Kontoe S, Taborda DMG, Tsiampousi A (eds)

https://doi.org/10.53243/NUMGE2023-252

The role of soil constitutive model in simulation of cone penetration test

S. Moshfeghi[1], M. Taiebat[1], A. Lizcano[2]

[1]*Department of Civil Engineering, University of British Columbia, Vancouver, BC, Canada*
[2]*SRK Consulting Inc., Vancouver, BC, Canada*

ABSTRACT: We present a detailed cone penetration test (CPT) simulation in which we use a Material Point Method (MPM) as a large deformation analysis platform and a base version of the SANISAND family of models as the soil constitutive model. This material model follows the framework of bounding surface plasticity with kinematic hardening of yield surface and critical state soil mechanics concepts, allowing a unified description of any pressure and density by the same model constants. Through a comparative study, we illustrate the importance of the soil constitutive ingredients by repeating the simulation using simplified versions of the constitutive model down to a basic nonlinear elastic-perfectly plastic model with Drucker-Prager yield surface and zero dilation. The results allow for appreciating the role of the soil model in the simulation of CPT. Selected details of this comparative study are presented and discussed in the paper.

Keywords: cone penetration test; constitutive model; SANISAND; material point method.

1 INTRODUCTION

The Cone Penetration Test (CPT) is a widely used in-situ test in geotechnical engineering to characterize soil, with a wide range of applications. However, the interpretation and characterization approaches based on CPT have some limitations due to the empirical nature of these correlations. Recent detailed numerical simulations of CPT have helped improve these correlations, leading to more accurate interpretation approaches (Ghasemi et al., 2018; Jia et al., 2021; Zhang et al., 2021). Accurate simulation of CPT requires two crucial components: representative constitutive models that can capture the nonlinear response of soil and a robust computational method capable of handling large deformation problems.

The Material Point Method (MPM) is a continuum-based numerical framework, originally proposed by Sulsky et al. (1994, 1995) that combines the benefits of point-based methods and mesh-based procedures, making it suitable for large deformation simulations (Fern et al., 2019). It is well-suited for large deformation problems, such as CPT process. Some recent studies have employed the MPM framework to simulate cone penetration, yielding promising results (e.g., Bisht et al., 2021; Ceccato et al., 2016; Martinelli and Galavi, 2021; Yost et al., 2022). These examples demonstrate the potential of MPM to accurately simulate cone penetration. Ongoing studies in this field include assessments in a range of drainage conditions and material types, including both fine- and coarse-grained soils.

Kouretzis et al. (2014a,b), through their study of numerical modeling of CPT based on an Arbitrary Lagrangian-Eulerian (ALE) remeshing technique, and a critical state sand model that followed the hardening law of Modified Cam-Clay model, emphasized the importance of the soil constitutive model used in the simulations. The constitutive model is expected to capture the dependence of cone resistance on the effective stress, relative density, and compressibility characteristics of the soil deposit. Furthermore, due to the large shear strains experienced by the soil during cone penetration, it is crucial to use advanced soil constitutive models that respect the critical state soil mechanics framework, for a realistic stress-strain response. Bisht et al. (2021), in their study on numerical modeling of CPT based on MPM, and a bounding surface constitutive model for clays, also pointed out the importance of using an adequate constitutive model for such simulations, highlighting the key relevant aspects of clay behavior: (a) the response during consolidation, including loading-unloading curves in the void ratio-mean effective stress space, (b) the transition from peak to residual state, and (c) the strain-rate dependency. Although these factors hold true for predominantly clay-like soils, one needs to account for additional key features when dealing with sand- and silt-type soils, as well as tailings, where the response can be more intricate. In such cases, the material state, which includes stress level, void ratio, and various fabric measures, plays a crucial role in determining the contractancy/dilatancy and hardening/sof-

tening response when subjected to the shear loading experienced during CPT. Bounding surface models have proven reasonable success in handling stress-strain nonlinearity. Other factors, such as fabric and anisotropic hardening, and adequate flow rule for accounting for material shear-volume coupling, are expected to be of key importance in modeling of CPT.

The aim of this paper is to evaluate the importance and role of the constitutive model in simulating CPT in dry sand. To achieve this, simulations were conducted using the DM04 sand plasticity model and within the MPM-based platform Anura3D. Under the same initial overburden stress, these simulations were carried out for two initial void ratios, representing Dense of Critical (DoC) and Loose of Critical (LoC) states. Subsequently, the DM04 model was simplified to a nonlinear elastic-perfectly plastic model with the Drucker-Prager yield surface and zero dilation, referred to as DP model here. Repeating the simulations using the DP model with different sets of parameters allows for assessing the effects of the deactivated model features. The results were presented and compared, and the impact of the constitutive model on the simulated cone tip resistance and the stress paths for a control material point is illustrated.

2 CONSTITUTIVE MODEL

The constitutive model used in this study is the well-known stress-ratio controlled, critical state compatible, bounding surface plasticity model proposed by Dafalias and Manzari (2004), often referred to as DM04 model, which formed the basis of what was later named SANISAND class of models (Taiebat and Dafalias, 2008). The model accounts for material anisotropy by incorporating the Lode angle dependency of the reference surfaces, including critical stress ratio, dilatancy stress ratio, and bounding stress ratio, and also by kinematic hardening of the yield surface.

The plastic module and dilatancy of the model are informed by the concept of state parameter $\psi = e - e_c$, where e and e_c refer to the current void ratio and critical state void ratio corresponding to the current mean effective stress p, respectively. This feature, in principle, is designed to allow for modeling the hardening/softening and contractancy/dilatancy aspects of response for different states of the material. Depending on the sign of ψ the model adjusts the reference bounding and dilatancy stress ratios, which in turn affects the corresponding distances to the stress ratio. These distances, together with the model constants h_0 and A_0, control the plastic modulus and dilatancy, respectively. At $\psi = 0$, the bounding and dilatancy surfaces collapse onto the fixed critical state surface, i.e., the critical state ratio in $p - q$ space. Additionally, the model incorporates a fabric dilatancy tensor that accounts for the fabric changes during plastic dilation and its effect on the subsequent contraction upon reverse loading, a relevant feature for dealing with cyclic shearing.

Table 1. Adopted model constants for DM04 and DP

Description	Symbol	DM04*	DP (Set 1)	DP (Set 2)
Elasticity	G_0	125	125	125
	ν	0.05	0.05	0.05
Critical state	M_c	1.25	1.25	1.6
	M_e	0.89	1.25	1.6
	λ_c	0.019	0.019	0.019
	e_{c_ref}	0.934	0.934	0.934
	ξ	0.7	0.7	0.7
Yield surface	m	0.01	1.25	1.6
Plastic modulus	h_0	7.05	0	0
	c_h	0.968	-	-
	n_b	1.1	-	-
Dilatancy	A_0	0.704	0	0
	n_d	3.5	-	-
Fabric dilatancy	z_{max}	4	-	-
	c_z	600	-	-

* For Toyoura sand, from Dafalias and Manzari (2004)

The model formulation follows a generalized multiaxial tensorial form, making it well-suited for application in various loading conditions. The model parameters can be calibrated in a fairly straightforward manner using standard types of laboratory tests. For example, drained and undrained triaxial compression and extension tests at different values of initial void ratio and confining pressure allow for calibrating different features of hardening/softening and dilatancy/contractancy of the model, with a step-by-step calibration process presented in Taiebat et al. (2010). Previous studies have demonstrated the model's efficiency for large deformation simulations (Staubach et al., 2021; Lino Ramírez, 2021).

The hierarchical design of the DM04 formulation allows for deactivating some of the model's key features by setting certain values to the controlling model constants. With this approach, one can reduce the DM04 to the basic elastic-perfectly plastic DP model with zero dilation, and only nonlinear elasticity. In particular, four model parameters need to be adjusted for this purpose: (i) using the same slope for the critical state in both tension and compression, by setting $M_e = M_c$; (ii) expanding the isotropic size of the yield surface to that of the critical state surface by setting $m = M_c$; and (iii) and (iv) deactivating the kinematic hardening and dilatancy by setting $h_0 = 0$ and $A_0 = 0$, respectively.

Table 1 presents the parameters for both the DM04 and DP models. Three sets of model constants were examined: (1) the full set of parameters of DM04 with the parameters presented in the original reference for

Table 2. Summary of simulations

Simulation ID	Model parameters	Initial void ratio (e_0)
I	DM04	0.654
II	DM04	0.950
III	DP (Set 1)	0.654
IV	DP (Set 1)	0.950
V	DP (Set 2)	0.654

Toyoura sand; (2) the simplified parameters that represent DP with the same strength as the DM04 model at critical state, referred to as Set 1; and (3) the simplified parameters that represent Drucker-Prager with the same strength as the DM04 model at the peak state for the DoC case in the triaxial drained test, referred to as Set 2. With these parameters, two different initial void ratios of 0.654 and 0.95 were selected to represent a dense of critical state (DoC) and a loose of critical state (LoC), respectively. The combined use of the material parameters listed in Table 1 for the DM04 and the DP models, and the two representative initial void ratios, set the basis for five simulations listed in Table 2; these simulations will be further elaborated below.

To better illustrate how these sets of model parameters and initial void ratios influence the stress-strain response, the combined sets of model parameters and initial void ratios listed in Table 2 were used to carry out five simulations of the conventional drained triaxial compression loading, as illustrated in Figure 1. The figure shows that DM04 with the full set of parameters in simulations I and II shows a nonlinear response involving hardening and softening, and also contraction and dilation depending on the material state, and the response tends to asymptotically go to the critical state. Simulations III and IV show nearly the same elastic-perfectly plastic response, with a minor difference in the elastic response; this is related to the state-dependent nonlinear elasticity in DM04, which results in the elastic shear modulus of the simplified DP being void ratio-dependent. The shear strength in these simulations nearly matches that of the critical state for simulations I and II. Finally, simulation V shows an elastic-perfectly plastic response but with a shear strength matching the peak shear strength shown in simulation II.

3 CPT MODEL DESCRIPTION

A 2D-axisymmetric numerical model was developed using the ANURA3D platform (Anura3D, 2022) to investigate the soil response to cone penetration. The model width was determined to be 0.32 m, which is around 20 times the cone radius ($20\,r_c$) based on preliminary sensitivity studies. The height of the soil domain was set to 1.0 m, and the cone penetration depth was limited to 0.4 m in order to avoid any effect from the bottom boundary on the results. The model boundary conditions included vertical and horizontal displacement constraints at both the top and the bottom boundaries. For the left and right boundaries, horizontal displacements in the direction normal to the boundary was fixed. An overburden stress of 110 kPa was applied at the soil top, and stresses were initialized using the K_0 procedure with the K_0 value of 0.5. In accordance with standard cone specifications, the cone had the radius of 3.17 cm with an apex angle of 60 degrees and was embedded in the soil to the depth of 3.75 cm. To prevent numerical instabilities, the tip of the cone was slightly rounded at its connection to the shaft. The cone was modelled as a rigid body; hence no stress-strain relationship was considered for the cone material points, and the cone only moved downward at the prescribed velocity. The contact between the cone and soil was

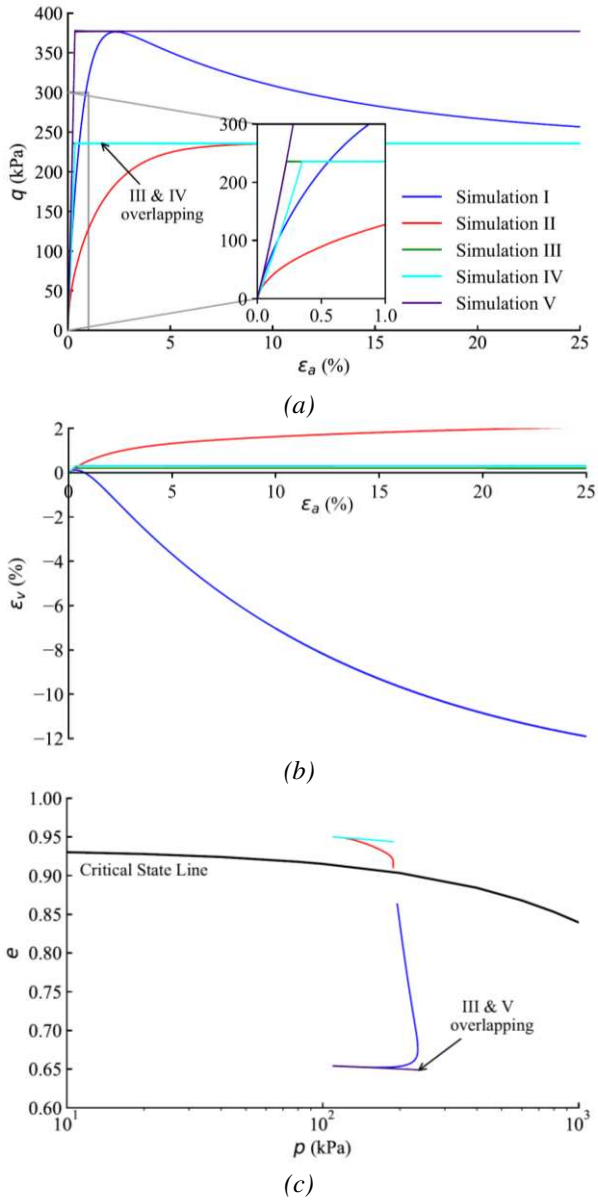

Figure 1. Stress paths for drained triaxial test simulations using three sets of model constants for the cases of dense and loose of critical

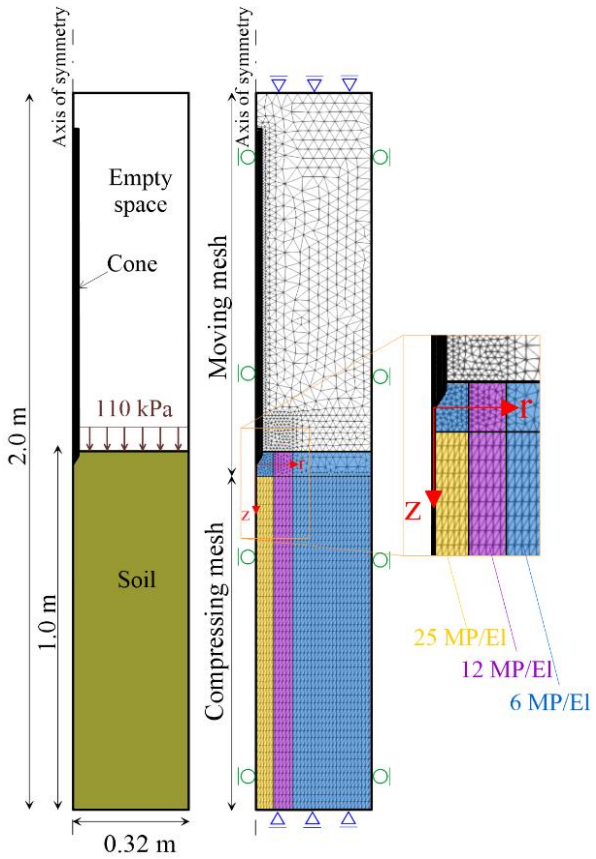

Figure 2. Numerical model configuration

governed by the algorithm proposed by Bardenhagen et al. (2001), with an interface friction angle of 31.5 degrees. Figure 2 illustrates the configuration of the model and additional details, including the dimensions, reference coordinate system at the cone tip, boundary conditions, compressing and moving mesh, discretization, and the number of material points per element (MP/EL) in different parts of the soil domain.

To reduce stress oscillations, the homogenous local damping of 10% was employed. Furthermore, to prevent the locking of elements, the strain smoothing technique proposed by Al-Kafaji (2013) was used. The DM04 model numerical implementation follows the Runge-Kutta-Dormand-Price integration scheme. To ensure accurate numerical integration of the DM04 model, a time increment of 1E-4 sec was chosen for all simulations. This decision was based on several factors, including the assigned penetration velocity of 2 cm/sec, the critical time step of approximately 0.5E-3 sec resulting from the chosen discretization and material model stiffness, and the need to guarantee adequate numerical integration.

The moving mesh technique was used for spatial discretization. This technique maintains a fine mesh around the cone tip throughout the simulation and ensures a well-defined geometry in the contact zone between the cone and soil, making computations more efficient (Al-Kafaji, 2013). A finer mesh was used at closer distances to the centreline of the cone, while the mesh became coarser further away from the cone to reduce computational cost. The boundary between moving and compressing mesh is located 15 cm below the top of the soil (12 cm below the cone tip).

The number of material points per element is a critical factor in ensuring that no empty elements are present during simulation, which could lead to errors in the final output. Additionally, a higher resolution is preferred in the vicinity of the cone. Therefore, the number of material points per element in the soil close to the cone tip was set to 25 MP/El. To reduce the computational cost, the number of material points per element was reduced to 12 and 6 in the zones progressively further from the centreline of the cone. A specific material point was selected as a control point to study the stress paths and soil state evolution during cone penetration. The initial location of the control material point (CMP) was at a depth of $z = 19\, r_c$, and a radial distance of $r = 1.1\, r_c$ from the cone tip.

4 RESULTS AND DISCUSSION

Figure 3 presents the cone tip resistance values obtained from all five simulations. The values were determined based on the vertical reaction forces recorded at the cone tip during the penetration process. It should be noted that the penetration depth z reported in this and subsequent figures is with measured respect to the cone tip at the start of the penetration, based on the coordinate system shown in Figure 2. This excludes the initial embedment of 3.75 cm below the soil surface.

The results show that for the DoC case, the cone tip resistance values from Simulation I (DM04) lie between

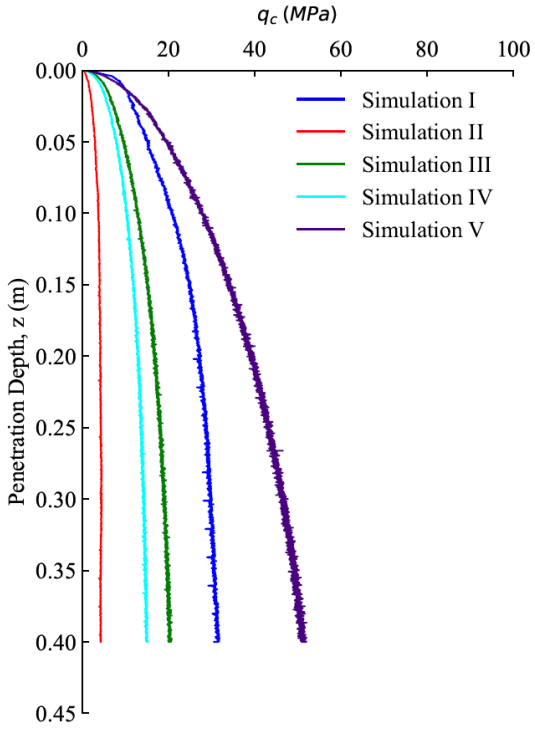

Figure 3. Cone tip resistance for all five simulation.

the values obtained from Simulation III (DP with Set 1) and Simulation V (DP with Set 2). Similarly, for the LoC case, Simulation II (DM04) and Simulation IV (DP with Set 1) yield different cone tip resistance values. Additionally, the cone resistance for Simulations III and IV, i.e., the LoC and DoC cases with the same sets of DP parameters, are slightly different due to nonlinear elasticity in the DM04 model, which depends on the void ratio. Thus, even when using simplified parameters, the elasticity part still varies with the initial void ratio, although the plastic part is void ratio independent. This leads to differences in the measured cone resistance.

These results illustrate that the cone tip resistance is not solely dependent on the critical state or peak strength, but is also influenced by the stiffness, hardening process, and the shear/volumetric coupling. In other words, the observed differences between the cone tip resistances obtained using the DM04 and the DP models highlights the critical role played by the features of the constitutive model in simulating the behaviour of dry sand during cone penetration. This underscores the inadequacy of relying solely on final critical state strength as a predictor of soil response. Therefore, it is essential to account for the elasticity, hardening/softening process, and contractancy/dilatancy aspect of response that soil undergoes during cone penetration to obtain a more accurate simulation of the cone resistance. This observation is also in line with the early work done by Shuttle and Jefferies (1998) on interpreting CPT data using cavity expansion theory, in which the effects of stiffness and hardening process were highlighted.

To investigate the response of the DM04 model in the cone penetration process, stress paths and state variable evolutions for the CMP were studied in further detail, as shown in Figure 4 for the simulations using DM04, i.e., Simulations I and II. It is observed that in the $e-p$ space, shown in Figure 4, as the penetration occurred, the soil state moved towards the projection of the critical state line on this space. The figure also highlights the start and end of the simulation and the moment when the cone tip reaches the CMP.

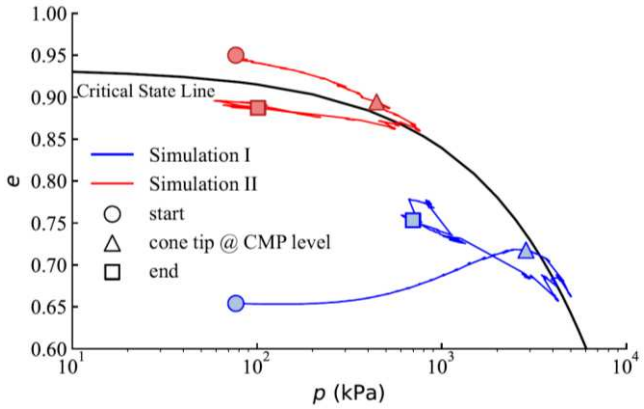

Figure 4. Variations of the material state in e-p space at the CMP for Simulations I and II

To comment on whether or not the soil has reached the critical state, one needs to examine whether mean pressure p, void ratio e, and stress ratio η (q/p) have reached the critical state simultaneously. The evolutions of the state variables of p and η with respect to their corresponding critical values, i.e., p_c and M_{CSL}, respectively, are shown in Figure 5. Also, the location of the CMP, i.e., at the normalized depth of $z/r_c = 19$, and where the state parameters nearly reached their critical values, i.e., at around $z/r_c = 20.5$, are highlighted in the insets of Figures 5(a,b). It can be inferred from these plots that when the tip of the cone reaches the elevation of the CMP, the material state at the CMP has not yet reached the critical state. However, shortly after that, and as soon as the cone shoulder reaches the depth of the CMP, the material state at the CMP nearly reaches the critical state. This contributes to obtaining different values of the cone resistance when using DM04 and DP, even with the same critical state strength value, as the cone tip resistance is measured at the tip of the cone where the material has not yet reached the critical state.

It is worth noting that as the cone tip passed the elevation of the CMP, some significant oscillations were observed in the stress variations. Assessing the reasons behind these stress oscillations and the remedy for those are being studied, and the findings will be discussed in a more extended version of the work.

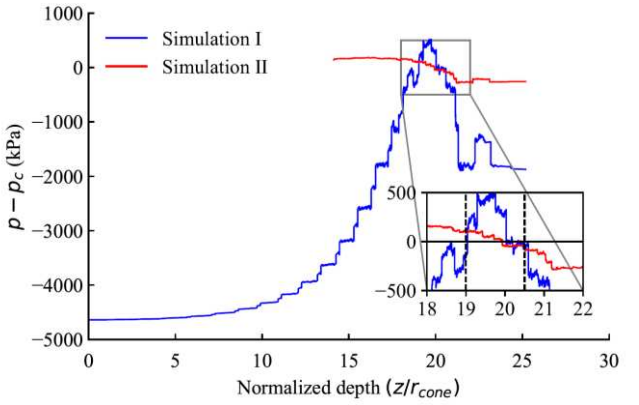

(a)

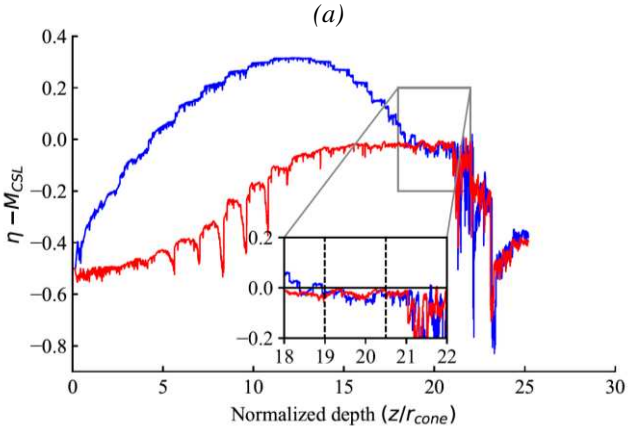

(b)

Figure 5. Variations of the material state with respect to the critical state at the CMP for Simulations I and II

5 CONCLUSIONS

The simulation of cone penetration in dry sand was presented using the material point method. To emphasize the significance of selecting the necessary constitutive model features, a base version of the SANISAND family of models (DM04) was utilized, along with its simplified version down to an elastic-perfectly plastic model with Drucker-Prager yield surface and zero dilation. Representative simulations were carried out using selected sets of model parameters and initial values of the material void ratio.

The results demonstrated that the DM04 model's features, such as nonlinear elasticity, hardening/softening rules, contractancy/dilatancy, and critical state-based framework of the model, play important roles in simulating the non-linear and anisotropic soil response. This, in turn, has an impact on cone penetration simulation results. The study confirmed that considering only the peak or critical state strength of the material alone is not the only characteristic affecting cone tip resistance. Rather, the soil's stiffness and the stress path experienced during the penetration process significantly affect the recorded cone tip resistance as well.

6 ACKNOWLEDGEMENTS

Support for this study was provided by the Natural Sciences and Engineering Research Council of Canada (NSERC) and SRK Consulting Inc.

7 REFERENCES

Al Kafaji, I.K., 2013. Formulation of a dynamic material point method (MPM) for geomechanical problems. Ph.D. thesis, Dept. of Civil and Environmental Engineering, University of Stuttgart.

Anura3D. 2022. Anura3D MPM research community. Online-External Workshop & Official Release, accessed on April 22, 2022, http://www.anura3d.com/.

Bardenhagen, S.G., Guilkey, J.E., Roessig, K.M., Brackbill, J.U., Witzel, W.M. and Foster, J.C., 2001. Improved contact algorithm for the material point method and application to stress propagation in granular material. Comput. Modell. *Engineering Science*, **2(4)**, 509-522.

Bisht, V., Salgado, R. and Prezzi, M., 2021. Material point method for cone penetration in clays. *Journal of Geotech and Geoenv Engineering*, **147(12)**, 04021158.

Ceccato, F., Beuth, L., Vermeer, P.A. and Simonini, P., 2016. Two-phase material point method applied to the study of cone penetration. *Computers and Geotechnics*, **80**, 440-452.

Dafalias, Y.F., Manzari, M.T., 2004. Simple plasticity sand model accounting for fabric change effects. *Journal of Engineering Mechanics*, **130(6)**, 622-634.

Fern, J., Rohe, A., Soga, K. and Alonso, E., 2019. *The material point method for geotechnical engineering: a practical guide*. CRC Press.

Ghasemi, P., Calvello, M., Martinelli, M., Galavi, V. and Cuomo, S., 2018. MPM simulation of CPT and model calibration by inverse analysis. In *Cone Penetration Testing,* 295-301, CRC Press.

Jia, R., Zhao, D., Lei, H. and Li, Y., 2021. Numerical study of the effect of clay structure on piezocone penetration test results. *International Journal of Geosynthetics and Ground Engineering*, **7**, 1-14.

Kouretzis, G.P., Sheng, D. and Wang, D., 2014a. Numerical simulation of cone penetration testing using a new critical state constitutive model for sand. *Computers and geotechnics*, **56**, 50-60.

Kouretzis, G.P., Sheng, D.C. and Wang, D., 2014b. Numerical simulation of CPT cone penetration in sand. In *Applied Mechanics and Materials*, **553**, 416-421, Trans Tech Publications Ltd.

Lino Ramírez, E.A. 2021. Modeling of flow liquefaction and large deformations in tailings dams using material point method. Master‘s Thesis, University of British Columbia.

Martinelli, M. and Galavi, V., 2021. Investigation of the material point method in the simulation of cone penetration tests in dry sand. *Computers and Geotechnics*, **130**, 103923.

Shuttle, D. and Jefferies, M., 1998. Dimensionless and unbiased CPT interpretation in sand. *International Journal for Numerical and Analytical Methods in Geomechanics* ***22*****(5)**, 351-391.

Staubach, P., Machaček, J. and Wichtmann, T., 2021. Large-deformation analysis of pile installation with subsequent lateral loading: SANISAND vs. Hypoplasticity. *Soil Dynamics and Earthquake Engineering*, **151**, 106964.

Sulsky, D., Chen, Z., Schreyer, H.L., 1994. A particle method for history-dependent materials. *Computer Methods in Applied Mechanics and Engineering*, **118(1-2)**, 179-196.

Sulsky, D., Zhou, S.J., Schreyer, H.L., 1995. Application of a particle-in-cell method to solid mechanics. *Computer Physics Communications*, **87(1-2)**, 236-252.

Taiebat, M., Dafalias, Y.F., 2008. SANISAND: simple anisotropic sand plasticity model. *International Journal of Numerical and Analytical Methods in Geomechanics* **32(8)**, 915-48.

Taiebat, M., Jeremić, B., Dafalias, Y.F., Kaynia, A.M., Cheng, Z. 2010. Propagation of seismic waves through liquified soils. *Soil Dynamics and Earthquake Engineering*, **30(4)**, 236-257.

Yost, K.M., Yerro, A., Green, R.A., Martin, E., Cooper, J., 2022. MPM modeling of cone penetrometer testing for multiple thin-layer effects in complex soil stratigraphy. *Journal of Geotechnical and Geoenvironmental Engineering*, **148(2)**, 04021189.

Zhang, W., Zou, J.Q., Zhang, X.W., Yuan, W.H. and Wu, W., 2021. Interpretation of cone penetration test in clay with smoothed particle finite element method. *Acta Geotechnica*, **16(8)**, 2593-2607.